

High-Resolution Mass Spectrometry Based Proteomic Analysis of the Response to Vancomycin-Induced Cell Wall Stress in *Streptomyces coelicolor* A3(2)

Andy Hesketh,^{*,†,‡} Michael J. Deery,^{†,‡} and Hee-Jeon Hong^{*,†}

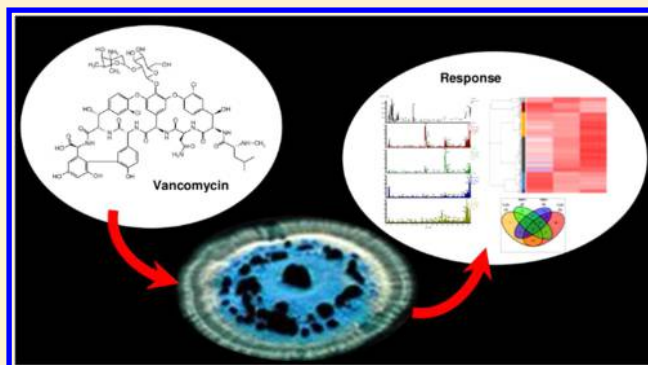
[†]Department of Biochemistry, University of Cambridge, Cambridge, U.K.

[‡]Cambridge Systems Biology Centre, University of Cambridge, Cambridge, U.K.

S Supporting Information

ABSTRACT: Understanding how bacteria survive periods of cell wall stress is of fundamental interest and can help generate ideas for improved antibacterial treatments. In this study we use tandem mass tagging to characterize the proteomic response of vancomycin resistant *Streptomyces coelicolor* to the exposure to sublethal levels of the antibiotic. A common set of 804 proteins were identified in triplicate experiments. Contrasting changes in the abundance of proteins closely associated with the cytoplasmic membrane with those taking place in the cytosol identified aspects of protein spatial localization that are associated with the response to vancomycin. Enzymes for peptidoglycan precursor, mycothiol, ectoine and menaquinone biosynthesis together with a multisubunit nitrate reductase were recruited to the membrane following vancomycin treatment. Many proteins with regulatory functions (including sensor protein kinases) also exhibited significant changes in abundance exclusively in the membrane-associated protein fraction. Several enzymes predicted to be involved in extracellular peptidoglycan crossbridge formation became significantly depleted from the membrane. A comparison with data previously acquired on the changes in gene transcription following vancomycin treatment identified a common high-confidence set of changes in gene expression. Generalized changes in protein abundance indicate roles for proteolysis, the pentose phosphate pathway and a reorganization of amino acid biosynthesis in the stress response.

KEYWORDS: *Streptomyces coelicolor*, vancomycin, cell wall stress, proteome, transcriptome



INTRODUCTION

For the last four decades vancomycin has been one of the antibiotics of choice for treating methicillin-resistant staphylococcal infections in the clinic,^{1,2} and also sees important use in the treatment of both amoxicillin-resistant enterococci and enteric *Clostridium difficile* infections.³ Resistance to vancomycin in clinically relevant pathogenic bacteria first emerged in enterococci in the 1980s⁴ followed ten years later by resistance in *Staphylococcus aureus* (reviewed in Howden et al.⁵). Vancomycin resistance is however an ancient property of some soil-dwelling bacteria where mechanisms evolved in antibiotic-producing strains (e.g., *Nonomurea*, *Amycolopsis* and *Streptomyces* species) for self-protection, and also in non-producing microbes presumably to enable them to compete more effectively with the producers in their environment.^{6–11} Evidence for the recent exchange of antibiotic resistance genes between environmental soil bacteria and clinical pathogens also illustrates that soil continues to be an important source for clinically relevant resistance determinants.¹² Investigating the signaling systems which coordinate the response to the presence of vancomycin or related antibiotics in soil bacteria

has been used as a way to understand aspects of the molecular mechanisms important for resistance,^{13–18} and contributes to our general understanding of how bacteria respond and adapt to environmental stresses. It has the potential both to provide novel insights into the mode of antibiotic action, and to suggest strategies for developing new anti-infectives.

We have previously undertaken an extensive analysis of the genome-wide transcriptional response in the Gram-positive soil bacterium *Streptomyces coelicolor* to three antibiotics, vancomycin, moenomycin A and bacitracin, targeting distinct stages of cell wall biosynthesis.¹⁹ *S. coelicolor* does not produce any glycopeptide antibiotic but harbors a cluster of seven genes conferring inducible resistance to vancomycin.⁷ The picture that emerged indicated a core common response to all three antibiotics involving activation of transcription of the cell envelope stress sigma factor σ^E , together with elements of the stringent response, and of the heat, osmotic and oxidative stress regulons, superimposed upon antibiotic-specific transcriptional

Received: March 20, 2015

Published: May 12, 2015

Table 1. TMT Mass Tagging of Protein Samples for Multiplex Relative Quantitation by LC–MS/MS

6-plex TMT tag	replicate 1	replicate 2	replicate 3
126	0 min; cytosol	0 min; cytosol	0 min; cytosol
127	45 min; cytosol	45 min; cytosol	45 min; cytosol
128	90 min; cytosol	90 min; cytosol	90 min; cytosol
129	0 min; membrane	0 min; membrane	0 min; membrane
130	45 min; membrane	45 min; membrane	45 min; membrane
131	90 min; membrane	90 min; membrane	90 min; membrane
total proteins quantified ^a	1057	1337	1335

^aNumber of different proteins represented by two or more peptides of sufficient quality to be quantified in the LC–MS/MS analysis.

changes representing cellular processes potentially important for tolerance to individual antibiotics. In this study we seek to more fully define the response induced by exposure of *S. coelicolor* to vancomycin by quantifying changes induced in the proteome. Fractionation of cell extracts into cytosolic and membrane protein components followed by high resolution LC–MS/MS analysis enabled changes in the abundance of proteins closely associated with the cytoplasmic membrane to be contrasted with those taking place in the cytosol, thus maximizing the information obtained about the response. Proteins targeted to the cytoplasmic membrane in bacteria fulfill roles that require more intimate contact with the external environment than gene products remaining in the cytoplasm, and identification and quantification of changes in their abundance can consequently provide a unique view of any response to external stress. This work represents one of only a limited number of studies aimed at characterizing the changes induced in a bacterial proteome in response to antibiotic stress using LC–MS/MS,^{20–22} and is the first analysis of the effect of vancomycin on the proteome of *S. coelicolor*.

MATERIALS AND METHODS

Bacterial Strains and Culture Conditions

S. coelicolor M600, a prototrophic plasmid-free derivative of *S. coelicolor* A3(2), was cultured and subjected to vancomycin stress using the method previously described in the transcriptome study.¹⁹ Briefly, spores were germinated and batch cultured in biological triplicate to mid log phase ($OD_{600\text{ nm}} \sim 0.5$) in NMMP medium. Cells were then exposed to a sublethal concentration (10 $\mu\text{g}/\text{mL}$) of vancomycin (Sigma), and samples taken 0, 45, and 90 min after addition of the antibiotic. Harvested cell pellets were flash frozen in liquid nitrogen then stored at $-80\text{ }^\circ\text{C}$ until use for protein sample preparation. Typically, mycelium from 50 mL culture samples was collected, with a transfer time from culture flask to frozen sample of 1.5 min. Data from the transcriptome study indicated that a 90 min sampling period adequately captures the immediate response to the antibiotic. A transient slowing in growth of the cultures was observed immediately following vancomycin addition, but the dose used is well below the minimum inhibitory concentration (MIC; $\sim 80\text{ }\mu\text{g}/\text{mL}$), and the cultures soon resumed a normal growth rate (doubling time $\sim 4\text{ h}$).

Protein Sample Preparation

Frozen cell pellets were resuspended in ice-cold wash buffer (50 mM Tris-HCl pH 7.6, 150 mM NaCl) then centrifuged at 4000 rpm for 1.5 min at $4\text{ }^\circ\text{C}$. Washed cells were transferred to 2 mL eppendorf tubes and resuspended on ice in a lysis buffer comprising 50 mM Tris pH 7.6, 5 mM DTT, 1 mM EDTA and complete protease inhibitor cocktail (Roche 11836170001). Cells were then lysed by sonication (10 \times 2 s bursts) while

cooling in an ethanol-ice bath, and cell debris removed by centrifugation (15 min, 10000g, $4\text{ }^\circ\text{C}$). The supernatant was separated into soluble and membrane fractions by ultracentrifugation (45 min at 150000g) at $4\text{ }^\circ\text{C}$, as previously reported in Kim et al.²³ After ultracentrifugation, soluble proteins in the supernatant were precipitated by addition of 6-volumes of ice cold acetone and overnight incubation at $-20\text{ }^\circ\text{C}$. Membrane pellets were subjected to a salt wash to remove nonspecifically associated proteins by resuspending them in wash buffer (above) containing 250 mM NaCl. Washed membranes were recovered by repeating the ultracentrifugation, and proteins extracted in lysis buffer (above) containing 1% SDS. Finally, the membrane-associated proteins were acetone precipitated as above.

Preparation of Tagged Tryptic Peptides for Multiplex Relative Quantitation by LC–MS/MS

Precipitated protein samples (100 μg) were processed and subjected to tandem mass tag (TMT) labeling using the Thermo Scientific (Waltham, MA) 6-plex Isobaric Label Reagent Set (90068) according to the manufacturers' instructions. In brief, proteins were first reduced and alkylated, then digested with trypsin and finally labeled with the 126, 127, 128, 129, 130, and 131 isobaric tags. Labeled samples, defined in Table 1, were then combined and lyophilized before being desalted using SepPak-C18 cartridges (Waters (Milford, MA)) and subjected to a preliminary fractionation using reverse-phase UPLC. Peptides, dissolved in 20 mM ammonium formate (pH 10.0) containing 4% (v/v) acetonitrile, were loaded onto an Acquity bridged ethyl hybrid C18 UPLC column (Waters (Milford, MA); 2.1 mm i.d. \times 150 mm, 1.7 μm particle size), and separated using a linear gradient of 5–60% acetonitrile in 20 mM ammonium formate (pH10.0) over 60 min at a flow-rate of 0.25 mL/min. Fractions were collected over 1 min intervals and reduced to dryness by vacuum centrifugation. Chromatographic performance was monitored in-line by sampling eluate with a diode array detector scanning between wavelengths of 200 and 400 nm.

Multiplex Relative Quantitation of Peptides by LC–MS/MS

Dried fractions from the high pH reverse-phase separations were dissolved in 30 μL of 0.1% formic acid and 1 μL aliquots analyzed by LC–MS/MS using a nanoAcquity UPLC (Waters (Milford, MA)) system and an LTQ Orbitrap Velos hybrid ion trap mass spectrometer (Thermo Scientific (Waltham, MA)). Reverse-phase separation of peptides was achieved by initially loading samples onto a UPLC Trap Symmetry C18 precolumn (Waters (Milford, MA), 80 μm i.d. \times 20 mm, 5 μm particle size) and eluting with 0.1% formic acid for 3 min at a flow rate of 10 $\mu\text{L}/\text{min}$. After this period, the column valve was switched to allow elution of peptides from the precolumn onto an analytical BEH C18 nano column (Waters (Milford, MA), 75

μm i.d. \times 250 mm, 1.7 μm particle size) eluting with a linear gradient of 5–30% acetonitrile in 0.1% formic acid over 60 min at flow rate of 300 nL/min. The LC eluant was sprayed into the mass spectrometer by means of a nanospray source, and m/z values of eluting peptide ions were measured in the Orbitrap Velos mass analyzer, set at a resolution of 30 000. To generate MS/MS spectra, Top-20 data dependent scanning was used to automatically isolate and generate fragment ions by higher-energy collisional dissociation (HCD) in the HCD cell, and the fragment ions passed into the Orbitrap (7500 resolution), via the C-trap, for mass analysis. Ions with charge states of 2+ and above were selected for fragmentation. An Isolation width of 1.2 Da was used for ion selection, and the normalized collision energy was 50% with a 2 step collision energy of 10%. A dynamic exclusion was applied with a repeat count of 3, repeat duration of 20 s and exclusion duration of 300 s.

Raw mass spectrometry data was processed to produce MS/MS peak lists in Mascot generic format using msconvert (ProteoWizard Project^{24,25}). Peptides were identified by querying peak lists with the Mascot search algorithm (v2.3.02, Matrix Science), using the *S. coelicolor* protein sequence database downloaded from StrepDB (<http://strepdb.streptomyces.org.uk>) in July 2011 (8218 sequences). A contaminant database (cRAP, <ftp://thegpm.org/fasta/cRAP>, 115 sequences) was also searched, and there was no overlap between contaminant ions (keratin and trypsin) and streptomyces peptide ions. TMT 6-plex (N-termini, K) and carbamidomethylation (C) were set as fixed modifications, and TMT 6-plex (Y) and oxidation (M) as variable modifications. Precursor and fragment ion mass tolerances were set to ± 25 ppm and ± 0.2 Da, respectively. Up to two missed tryptic cleavages were permitted. Peak lists were also queried against a “decoy” database of scrambled peptide sequences to estimate false discovery rates. Mascot search results from the forward and decoy database searches were then processed with Mascot Percolator, a machine learning algorithm that rescues peptide-spectrum matches (PSMs) to yield a more robust false discovery rate.²⁶ TMT reporter ions for PSMs with a posterior error probability of less than 0.01 were quantified using the i-Tracker algorithm,²⁷ yielding a list of identified proteins and associated TMT 6-plex quantification. The median spectral intensity quantitation value per PSM for each reporter ion, which is a robust method to remove outliers, was used to produce the protein-level abundances shown in Supporting File S1. The mass spectrometry proteomics data have been deposited to the ProteomeXchange Consortium (www.proteomexchange.org) via the PRIDE partner repository (<http://www.ebi.ac.uk/pride>) with the dataset identifier PXD002216.

Downstream Processing and Analysis of Proteomics Data

The protein-level quantitative data was filtered to remove proteins only represented by a single peptide, and then to remove those not quantified in all of the three replicate experiments. This produced a data set of 804 proteins. Within replicate normalization based on the isobaric TMT tags was performed by dividing row-wise by the mean of the three values for the 0, 45, and 90 min samples (and multiplying by 1000), treating the data from the cytosolic and membrane enriched protein fractions separately. After merging the data from all three replicates, abundance values were log₂ transformed to produce the normalized data. Raw and normalized protein abundance values are given in Supporting File S1.

To assess the relative distribution of each protein between the cytosolic and membrane-associated fractions, localization scores for each of the 804 proteins identified were calculated from the raw protein-level data as described in the Supporting Methods. The observed localizations as indicated by the localization scores were compared to predictions for the localization of gene products taken from the LocateP database²⁸ on January 15th 2015 (Supporting File S2).

To identify proteins differentially expressed in either the cytosolic or membrane fractions following vancomycin treatment, the normalized abundance data was analyzed by linear modeling using LIMMA,²⁹ applying a false discovery rate of adjusted $P < 0.05$. P -values were adjusted using the Benjamini and Hochberg multiple testing correction. Hierarchical clustering of abundance profiles was performed in R using the `hclust` function with Pearson correlation and complete linkage settings. Proteins exhibiting significantly different rates of change in abundance in the cytosolic subproteome compared to the membrane-associated subproteome were identified and classified as described in the Supporting Methods (Supporting Files S5 (45 min) and S6 (90 min)).

Gene ontology analysis (GO) was performed on lists of differentially expressed proteins to identify over-represented biological functions using the *S. coelicolor* GOA annotation from EBI-EMBL (84.S_coelicolor.goa) as listed on Jan 21st 2015. GO analyses were realized with the Ontologizer tool using the topology-weighted algorithm.³⁰

Integration of Proteome and Transcriptome Data

Normalized transcript abundance data from an analysis of the transcriptomic response of *S. coelicolor* to vancomycin performed using identical culture conditions to the present proteomics study was obtained from ArrayExpress submission E-MEXP-3032.¹⁹ The two data sets were integrated as described in the Supporting Methods. The transcript-protein congruence (TPC) coefficients calculated are a measure of the rate of change in protein abundance relative to the change in transcript abundance. A high TPC value implies that some mechanism is boosting protein abundance relative to the mRNA levels, and conversely a low coefficient means some mechanism is reducing the protein level relative to the mRNA.

RESULTS

LC-MS/MS Analysis of Proteins from Cytosolic and Membrane-Associated Fractions

A transcriptomic analysis has previously identified significant changes in the transcription of 1805 genes in the 90 min period immediately following treatment of exponentially growing cells of *S. coelicolor* with a subinhibitory concentration of vancomycin.¹⁹ To determine the extent to which this transcriptional response is carried through into changes in protein expression we have repeated this vancomycin stress experiment using identical conditions, and extracted protein samples for analysis by high-resolution mass spectrometry based quantitative proteomics using TMT 6-plex isobaric labeling.³¹ Vancomycin targets bacterial cell wall biosynthesis by binding and sequestering non-cross-linked peptidoglycan pentapeptide side chains (reviewed in Kahne et al.³²), and gene products located in the cell envelope are expected to play a significant role in responding to the presence of this antibiotic. To contrast changes in the abundance of proteins targeted to the cytoplasmic membrane with those remaining in the cytosol, cells harvested 0, 45, and 90 min after treatment with

vancomycin (10 $\mu\text{g}/\text{mL}$) were fractionated by ultracentrifugation to obtain cytosolic and membrane-associated protein samples for analysis. Isobaric labeling of the fractionated protein extracts from three biological replicate cultures using TMT 6-plex tags then permitted the simultaneous analysis of all six samples from each replicate experiment (Table 1). Postacquisition processing of the mass spectrometry data collected quantified 1057–1337 different proteins per replicate that were represented by data from at least two unique peptides (see Table 1).

A total of 804 proteins, equivalent to about 11% of the theoretical proteome, had quantitative data available from all three replicate experiments, and abundance values from this common set were used in all downstream analyses (Supporting File S1). The effectiveness of the preparation of the cytosolic and membrane subproteome fractions was assessed by calculating localization scores for each of the 804 proteins identified (see Materials and Methods), and comparing these observations with predictions obtained from the LocateP²⁸ database (Figure 1, Supporting File S2). The localization scores calculated from the data for the untreated samples (0 min) show a bimodal distribution with two peaks centered at 0.2 and 0.77 and exhibiting an area ratio of approximately 1:4 respectively (Figure 1a). Low scores indicate proteins detected predominantly in the membrane fraction (e.g., the lowest calculated score 0.03 for SCO3565, a predicted integral membrane protein possessing two predicted transmembrane helices), while proteins detected predominantly in the cytoplasm have high scores (e.g., 0.953 for SCO4165, a predicted hypothetical protein possessing no predicted transmembrane helices). The observed bimodal distribution is broadly consistent with the predictions from LocateP for the distribution of localizations within the data set of 804 proteins (Figure 1b). Proteins with low localization scores are dominated by those predicted to be membrane localized, and conversely, those with high localization scores are dominated by those predicted to be intracellular proteins. Proteins with intermediate localization scores around 0.5 could represent those resident in both fractions but could also be the result of limitations in the resolution of the fractionation procedure. Exceptions to the general trends also exist. Of the 184 proteins with a localization score less than 0.25, 70 are predicted by LocateP to be intracellular. However, 22 of these are predicted to interact with membrane bound ABC transport or membrane-associated multienzyme complexes (e.g., ATP synthase, succinate dehydrogenase), and 15 are ribosomal proteins, members of which family have previously been observed in bacterial membrane subproteomes.^{23,33} It is therefore possible that the remainder of the group of 70 genuinely localize to the membrane, and it is interesting to note that six are encoded by operons which also encode at least one putative transmembrane protein, and that there are five proteins (SCO4439, SCO2589–90, and SCO4246–47) with possible roles in cell envelope biosynthesis.

Significant Changes Are Induced in Both the Membrane-Associated and Cytosolic Subproteomes in Response to Vancomycin

High-level comparison of the protein abundance data using principal components analysis (PCA) indicates that exposure to vancomycin produced marked changes in both the cytosolic and membrane-associated subproteomes in *S. coelicolor* over the 90 min period (Figure 2a). Data for the cytosolic and

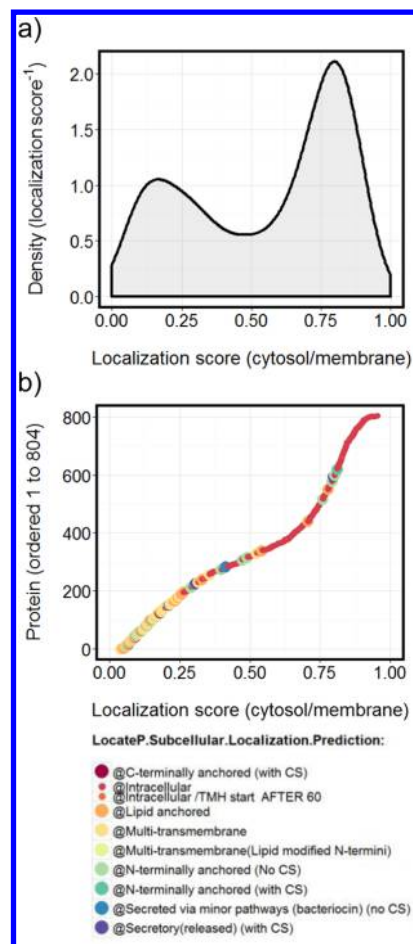


Figure 1. Comparison of the predicted and observed subcellular localizations for the 804 proteins quantified in the LC–MS/MS analysis. (a) Density plot for the localization score values calculated for each protein from the experimental observations obtained from the untreated cultures (immediately prior to vancomycin addition (0 min)). The score is a unitless value representing the proportion of protein present in the cytosolic sample relative to the membrane-associated sample such that a value of 1 would indicate a protein detected 100% in the cytosol and a value of 0 would indicate 100% detected in the membrane. (b) Comparison of the observed localization for each protein in the data set with localizations predicted from the amino acid sequence data using LocateP. Proteins are plotted by increasing localization score and colored according to their predicted LocateP localization group (LocateP.Subcellular.Localization.Prediction).

membrane protein fractions also clustered distinctly from each other as expected. Statistical analysis using LIMMA identified 314 proteins in the cytosolic fraction whose abundance was significantly different (at the 5% probability level) in the 90 min period following exposure to vancomycin, and 398 proteins from the membrane fraction (Figure 2b and Supporting Files S3 and S4). A total of 177 different proteins were shared between these sets, with 137 uniquely identified in the data from the cytosolic samples and 221 unique to the membrane-associated sample data.

Reassuringly, three of the seven proteins encoded by the vancomycin resistance gene cluster in *S. coelicolor* were identified in the proteomics analysis, VanA, VanK and VanH, and all were markedly (by at least 16-fold) and significantly up-regulated in both the cytosolic and membrane-associated protein extracts taken 90 min after vancomycin treatment

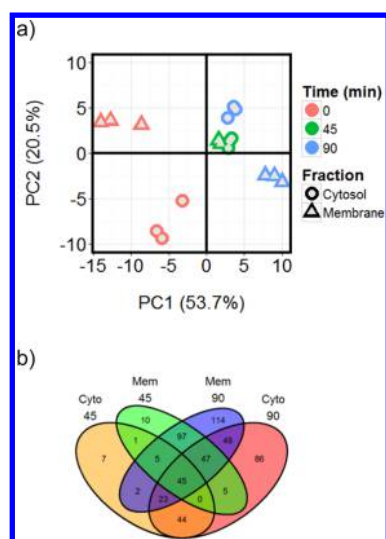


Figure 2. Changes induced in the *S. coelicolor* proteome following treatment with vancomycin. (a) PCA of the abundance of 804 proteins identified in high-resolution LC–MS analysis of membrane-associated and cytosolic protein fractions (PC1 and PC2 explain 74.2% of the variability in the data). (b) Summary of the proteins identified as being significantly differently ($P < 0.05$) expressed in the cytosolic protein fraction 45 (Cyto 45 (orange)) and 90 (Cyto 90 (red)) min after vancomycin addition, and similarly also in the 45 (Mem 45 (green)) and 90 (Mem 90 (blue)) min samples of the membrane-associated protein fractions.

(Supporting Files S3 and S4). Hierarchical clustering of the abundance profiles for all the proteins identified as significantly differently expressed broadly grouped the data into those proteins increasing in abundance following vancomycin treatment, and those decreasing in abundance (Figure 3 and Supporting File S4). GO analysis indicates that the proteins generally up-regulated in the cytosolic fraction are enriched in functions associated with arginine biosynthesis, response to stress, NADP-binding, oxidoreductase activity, proteolysis and the pentose-phosphate shunt pathway (Figure 3a). Down-regulated proteins in this fraction are enriched for manganese ion binding and peptidoglycan metabolic process GO categories. Similar analysis of the data for the membrane-associated samples reveals a different picture: up-regulated proteins are significantly enriched for proteins with functions associated with cellular protein catabolism, peptidoglycan metabolic process, and metal ion binding (including iron–sulfur cluster binding proteins); while down-regulated proteins are enriched for drug binding, protein folding and nitrogen compound transport processes (Figure 3b). Proteins from the peptidoglycan metabolic process GO term GO:0009252 are therefore significantly enriched in seemingly opposing categories: proteins down-regulated in the cytoplasm and those up-regulated in the membrane, suggesting a preferential enrichment for the peptidoglycan biosynthesis machinery at the cell envelope in response to vancomycin stress. These include enzymes responsible for the intracellular synthesis of the peptidoglycan precursor lipid II (SCO2084 MurG, SCO2088 MurF, SCO3904 FemX, SCO5560 DdlA and SCO6060 MurC; Figure 4). In contrast, homologous enzyme activities to FemX and DdlA that are encoded by the vancomycin resistance cluster (VanK and VanA, respectively) are markedly up-regulated in both the cytosolic and the membrane-associated subproteomes (Figure 4).

Contrasting Changes in the Membrane-Associated Proteome with Those Taking Place in the Cytosol Suggests an Element of Spatial Control in the Response to Vancomycin

In order to gain further insight into the relative changes in abundance of proteins in the cytosol and membrane subproteomes during the 90 min immediately following treatment of cells with vancomycin, the rate of change in abundance of each protein was tested for significant differences between the two fractions. We define the average rate of change of a protein after 45 min of treatment as $\log_2(A^{45}/A^{t0})$, and as $\log_2(A^{90}/A^{t0})$ after 90 min, where A^{t0} corresponds to the normalized abundance of the protein at the time of vancomycin addition, and A^{45} or A^{90} is the normalized abundance measured at the indicated time after treatment. Linear modeling was then used to identify proteins exhibiting significantly different rates of change in abundance between the two subproteomes. A positive value for the ratio of the relative change in the level of a protein in the cytosol to the relative change in the level of the same protein in the membrane-associated subproteome implies that it has been enriched in the cytosol relative to the membrane by a process of cytosol enrichment or membrane depletion. Conversely, proteins enriched in the membrane relative to the cytosol, by processes of membrane enrichment or cytosol depletion, would possess a negative value for the ratio. Final classification of proteins exhibiting significantly different changes in abundance between the two subproteomes as “cytosol enriched”, “membrane enriched”, “cytosol depleted”, or “membrane depleted” was achieved as defined in the Materials and Methods (Figure 5, and Supporting Files S5 and S6). Reassuringly, mapping of these classifications onto plots contrasting the protein localization scores between the 0, 45 and 90 min time points is entirely consistent with the assignments made (Supporting Figure S1).

GO analysis (Supporting Tables S1 and S2) indicates that the proteins found to be depleted from the membrane during the 90 min following exposure to vancomycin are enriched in functions linked to drug binding (4.53×10^{-4} ; SCO2608 *pbp2*, SCO3157, SCO3848, SCO3901, SCO4013) and Ser/Thr protein kinase activity (2.66×10^{-3} ; SCO2974 *pkaA*, SCO3848, SCO4775 *pkaH*). The former group comprise four predicted secreted penicillin-binding proteins (PBPs) putatively involved in cell wall biosynthesis plus the predicted Ser/Thr protein kinase encoded by the SCO3848 gene which is located immediately downstream from the PBP encoding gene SCO3847. The abundance of the proteins in both groups decreases by approximately 2-fold exclusively in the membrane subproteome during the course of the experiment (Figure 6a). In contrast, proteins found to be increasing in abundance exclusively in the membrane during the 90 min following exposure to vancomycin include those associated with the GO functions GTP binding (1.12×10^{-3} ; SCO1441, SCO1758, SCO2082, SCO2539, SCO2595, SCO4041, SCO4661, SCO5061, SCO6097), 4 iron–4 sulfur cluster binding (1.53×10^{-2} ; SCO0216, SCO2162, SCO4494, SCO4550, SCO5553, SCO5752, SCO5787), ectoine metabolic process (1.7×10^{-2} ; SCO1865, SCO1866, SCO1867) and nitrate metabolic process (2.88×10^{-2} ; SCO0216, SCO0217) (Figure 6b). Transcription of the ectoine biosynthesis cluster SCO1864–67 was previously shown to be significantly up-regulated in response to vancomycin,¹⁹ and this proteome study shows that three of the gene products are targeted preferentially to the membrane

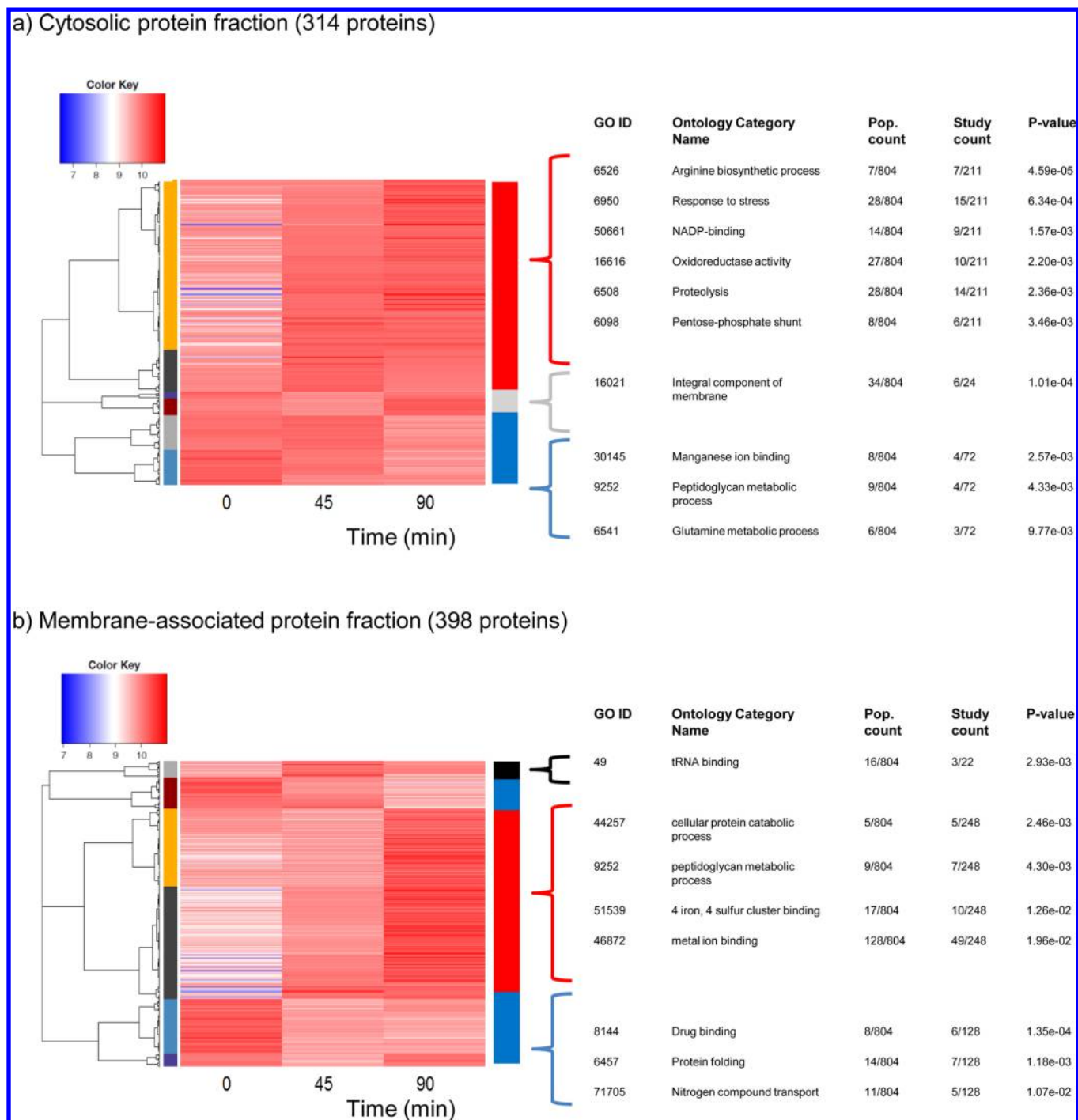


Figure 3. Hierarchical clustering of the proteins identified as significantly changing in abundance (corrected $P < 0.05$) in response to vancomycin in (a) the cytosolic and (b) the membrane-associated subproteome fractions. Clustering was performed in R using the `hclust` function with Pearson correlation and complete linkage settings (Supporting File S4). Clusters have been amalgamated into the groups indicated by the color bar on the right (red = up-regulated; blue = down-regulated; gray = transiently down-regulated; black = transiently up-regulated) and then subjected to GO analysis as described in the Materials and Methods. Significantly enriched GO terms are summarized in the tables shown.

compartment where they exhibit a 4-fold increase in abundance. Surprisingly, GO analysis of the proteins shown to be preferentially enriched in the cytosol following vancomycin treatment identified functional enrichment in the category “intrinsic component of the membrane” (1.10×10^{-2} ; SCO1515, SCO2155, SCO5369, SCO5695, SCO5580) (Supporting Table S2). Figure 6c suggests that these six membrane proteins, which include the cytochrome oxidase C subunit Cox1 (SCO2155) and the ATP synthase B chain AtpF

(SCO5369), increase in abundance in the cytoplasm while being lost from the membrane. Also increasing in abundance preferentially in the cytoplasm are proteins belonging to the response to stress GO category (1.12×10^{-2} ; SCO0641, SCO2367, SCO2368, SCO3661, SCO4277, SCO5494) which include the ATP-dependent protease ClpB, and four closely related homologous proteins SCO0641, SCO2367, SCO2368 and SCO4277 belonging to a family of tellurium resistance proteins.³⁴ Two enzymes assigned to the biosynthesis of the

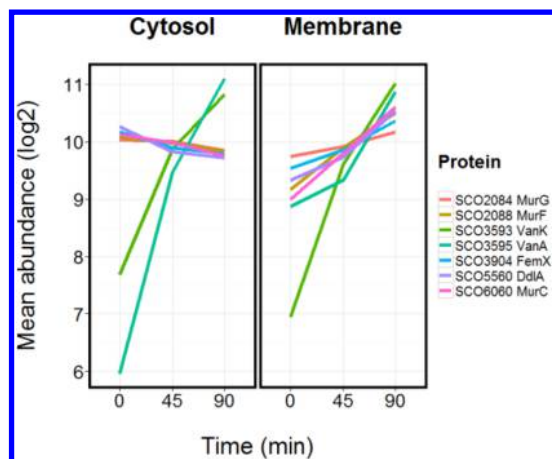


Figure 4. Mean normalized abundance profiles for the differentially expressed proteins belonging to the peptidoglycan metabolic process GO term (GO:0009252) showing an increase in abundance of MurG, MurF, MurC, DdlA and FemX exclusively in the membrane-associated subproteome following treatment with vancomycin. The VanK, VanH and VanA enzymes from the vancomycin resistance cluster show marked increases in abundance in both the cytosolic and membrane-associated fractions.

actinomycete-specific thiol buffer mycothiol³⁵ increased by approximately 2-fold only in the membrane subproteome 90 min after vancomycin treatment (Figure 6d). Three putative sensor histidine kinase proteins (SCO5748, SCO7422, SCO7463) also exhibited significant membrane subproteome-specific changes in abundance, and five putative transcriptional regulatory proteins (SCO1488, SCO2440, SCO3571, SCO3857, SCO6687) showed a significant increase in abundance (>2-fold) only in the membrane fraction (Figure 6e). SCO7422 and SCO7463 are histidine kinases belonging to two of the 13 conservons (conservons 10 and 13 respectively) identified in the *S. coelicolor* genome, and both show a ca. 2-fold

decrease in abundance exclusively in the membrane fraction in the 90 min following vancomycin treatment. Proteins from conservons 1, 2, 5, and 12 were also identified in this study, but of these only the histidine kinase CvnA1 (SCO5544) was identified as significantly changing in abundance, exhibiting a decrease in both the cytosolic and membrane fractions (see below). In contrast to SCO7422 and SCO7463, the OsaA histidine kinase encoded by SCO5748 shows a significant increase in abundance only in the membrane subproteome after vancomycin treatment. OsaA forms part of an osmotic stress response system.³⁶ Among the transcriptional regulators similarly showing an exclusive increase in abundance in the membrane fraction is the cyclic AMP receptor protein Crp (SCO3571) which has previously been implicated in the developmental processes of sporulation and germination.^{37,38}

The Two-Component Regulatory System Proteins CseBC and the Major Sigma Factor σ^{HrdD} Significantly Increase in Abundance in Response to Vancomycin

A central response to damage induced by a wide variety of cell-wall-damaging agents in *S. coelicolor* is coordinated by the CseBC- σ^{E} signal transduction system, ultimately via downstream effects on gene transcription directed by the alternative sigma factor σ^{E} .^{39,40} Transcription of the *sigE* gene however is completely dependent on a two-component system consisting of CseB, a response regulator, and CseC, a transmembrane sensor histidine protein kinase.⁴¹ CseB (SCO3358) and CseC (SCO3359) were significantly increased in abundance in both the cytosolic and membrane-associated subproteomes following exposure to vancomycin (Figure 7a). Peptides from the σ^{E} protein were not detected in this analysis, but the *sigE* gene is transcribed as part of a four gene *sigE-cseA-cseB-cseC* operon in which >90% transcription from the single *sigE* promoter terminates just downstream of *sigE*⁴¹ and the abundance of σ^{E} is therefore likely to have also increased along with the CseBC proteins. The abundance of the sigma factor σ^{HrdD} (SCO3202) also increased >4-fold in both subproteome fractions (Figure

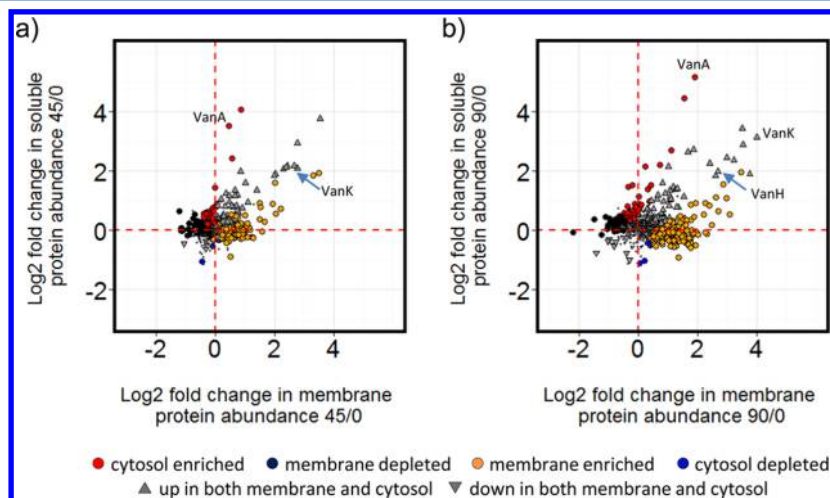


Figure 5. Contrasting the rate of change in abundance of proteins in the cytosolic and membrane-associated subproteomes of *S. coelicolor* following exposure to vancomycin for (a) 45 min, and (b) 90 min. Proteins exhibiting significantly different (corrected $P < 0.05$) rates of change in abundance are indicated by the large diameter circles, and have been further classified into the groups indicated by their color as described in the Supporting Methods (cytosol enriched, red circles; cytosol depleted, blue circles; membrane enriched, orange circles; membrane depleted, black circles). Significantly differently expressed proteins encoded by the vancomycin resistance cluster are indicated. Proteins showing no significant difference in their rate of change between the two fractions are indicated by small gray circles or large gray triangles. The large gray triangles correspond to proteins identified as being significantly and coordinately up-regulated (triangle apex oriented to the top) or down-regulated (triangle apex oriented to the bottom) in both fractions over the time period indicated (also see Supporting Files S5 and S6).

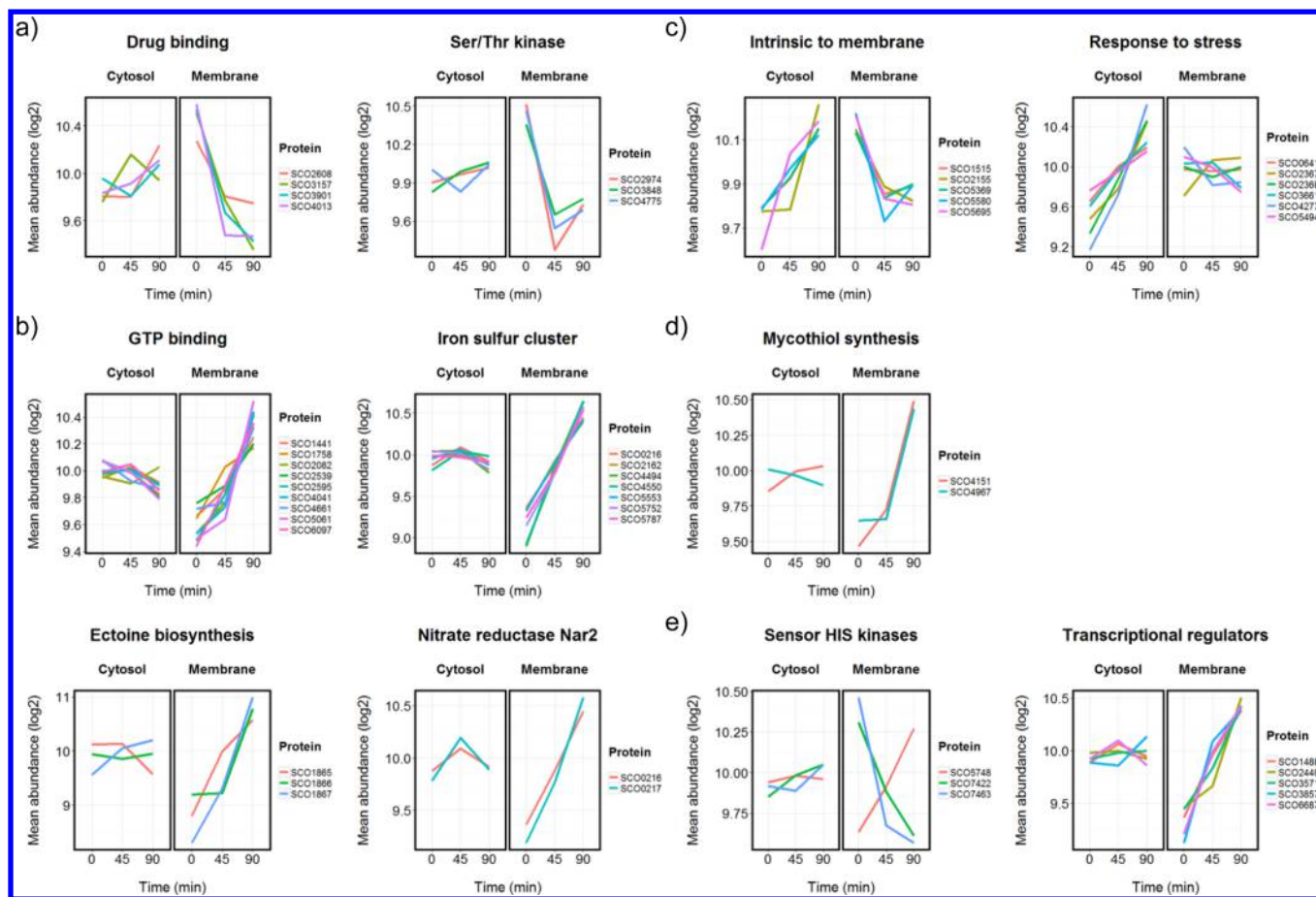


Figure 6. Mean normalized abundance profiles for selected groups of proteins identified from the analysis in Figure 5. (a) Proteins found to be depleted from the membrane subproteome but not the cytosol following exposure to vancomycin, grouped according to the significant GO category enrichment identified in Supporting Table S1. (b) Proteins found to be increasing in abundance in the membrane subproteome but not the cytosol, grouped according to the significant GO category enrichment identified in Supporting Table S1. (c) Proteins found to be increasing in abundance in the cytosol but not the membrane subproteome following exposure to vancomycin, grouped according to the significant GO category enrichment identified in Supporting Table S2. (d) Enzymes for mycothiol biosynthesis. (e) Proteins with predicted regulatory functions that exhibit significant changes in abundance in the membrane subproteome but not the cytosolic protein fraction.

7b) and it is interesting to note that σE controls transcription from one of the two promoters from which the σ^{HrdD} gene is transcribed.⁴¹ In contrast, the abundance of the major vegetative sigma factor σ^{HrdB} (SCO5820) significantly decreased following exposure to vancomycin, but only in the membrane subproteome (Figure 7b).

Seven additional proteins with putative regulatory functions were identified as being coordinately up-regulated in both the cytosolic and membrane-associated fractions: two related Ser/Thr protein kinase homologues PksC (SCO3821) and PksJ (SCO4779); and five putative DNA-binding transcriptional regulatory proteins (SCO0168, SCO0608, SCO2094, SCO3352, SCO7168) of unknown function (Figure 7c). In contrast, the histidine kinase CvnA1 (SCO5544) was coordinately down-regulated in both fractions, although exhibited a greater fold-change decrease in the membrane fraction (Figure 7c)

The Response to Vancomycin at the Transcript and Protein Levels Shows a Good Correlation on the Global Scale with Significant Exceptions for Individual Genes

To compare the response to vancomycin detected in the proteome with that previously reported for the transcriptome, transcript abundance measurements determined using Affyme-

trix microarrays were taken from Hesketh et al.¹⁹ and processed as described in the Materials and Methods section. Pearson correlation of the relative change in the level of each mRNA with the relative change in the level of its cognate protein present in the cytosolic fraction showed moderate to good positive correlation ($r = 0.51\text{--}0.65$; $p < 2.2 \times 10^{-16}$), while correlation with the membrane protein abundance values was also positive and significant but notably weaker ($r = 0.35\text{--}0.45$; $p \leq 2.18 \times 10^{-13}$) (Figure 8a). Transcript-protein congruence (TPC) plots comparing the changes in transcript abundance and protein abundance at the individual gene level for the cytosolic and membrane subproteome samples also indicate that there is good general agreement between the transcriptome and proteome measurements for the majority of the data over both the 45 and 90 min time periods, with most gene products exhibiting TPC coefficients between -1 and $+1$ for each sample set (Figure 8b and c). A combined total of 298 (37% of the 804) genes were however identified as deviating significantly from this trend in the cytosolic subproteome data, and 454 (56% of the 804) in the membrane subproteome (Supporting Files S7 and S8, respectively). Genes exhibiting changes in transcript abundance that correlate poorly with corresponding changes in abundance of the cognate protein can be indicative of the existence of post-transcriptional control

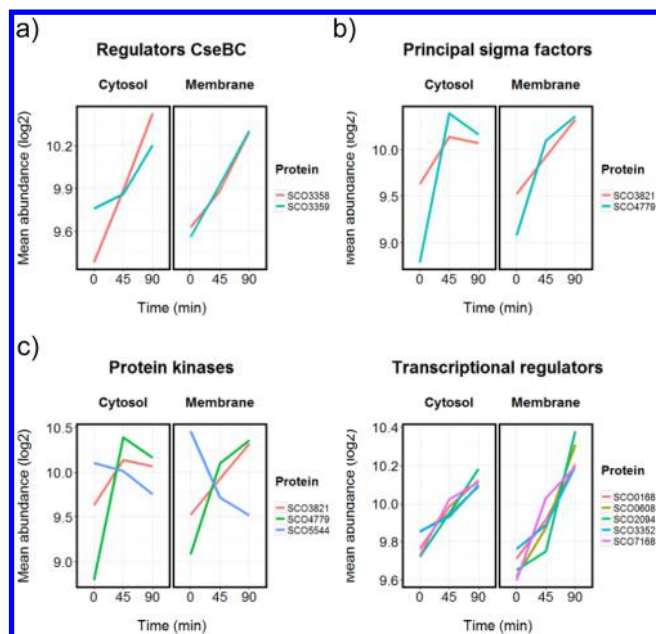


Figure 7. Mean normalized abundance profiles for selected groups of regulatory proteins identified from the analysis in Figure 5 and discussed in the text.

mechanisms regulating protein synthesis, but in the context of this study could also result from differential localization of the gene products between the cytosol and the membrane.

Genes commonly identified as differentially expressed in both the transcriptome and proteome data (Figure 8d) can be considered as a high-confidence set of vancomycin responsive genes in *S. coelicolor* and are listed in Supporting File S9. These include all the genes from the vancomycin resistance cluster for which there was protein abundance data available (*vanK*, *vanH*, *vanA*), and *hrdD*, *cseB* and *cseC*. GO analysis of these gene sets highlighted enrichment in previously identified categories and emphasized an up-regulation in the synthesis of proteins associated with protein catabolism (GO:00030163) which takes place in both the cytosolic (SCO1644 PcrB, SCO1647, SCO1648 Arc, SCO3404 FtsH2, SCO5285 Lon) and membrane (SCO1640, SCO1644 PcrB, SCO1647, SCO1648 Arc, SCO5285 Lon) subproteomes (Supporting Table S3).

DISCUSSION

Exposure of *S. coelicolor* to vancomycin resulted in extensive changes in both the cytosolic and membrane-associated subproteomes. The sample fractionation procedure was simple but was shown to be adequate for distinguishing proteins predicted to be resident in the cell membrane from those predicted to localize to the cytoplasm (Figure 1). Proteins observed to be more or less equally shared between the different fractions could be the result of nonspecific binding during isolation of the membranes, but could also indicate those gene products which localize to both subcellular areas. Previous proteomics analysis of *S. coelicolor* membrane proteins prepared using a more extensive washing procedure and sodium carbonate extraction also identified a population of proteins detectable in both the intrinsic membrane and cytosolic fractions, including enzymes from primary metabolism, ribosomal protein subunits, translational initiation cofactors and regulatory proteins.^{33,42} Fractionation and analysis of the subproteomes in *S. aureus* and *Bacillus subtilis*

similarly identified significant overlap between the residents of membrane and cytosolic samples.^{21,43} A consideration of the functional significance of the proteins changing in abundance following treatment with vancomycin indicates a response involving a marked reorganization of metabolism, as discussed in the following sections. These observations generate a number of new hypotheses that can be tested experimentally.

(i). Cell Wall Biosynthesis

The induction of enzymes from the vancomycin resistance cluster for the redirection of peptidoglycan precursor biosynthesis toward lipid II derivatives terminating in a D-Ala-D-Lac dipeptide in place of D-Ala-D-Ala was observed as expected (Figure 4), as was up-regulation of the CseBC two-component regulatory system involved in sensing and coordinating a response to cell envelope stress (Figure 7b). Interestingly, the membrane-associated subproteome also provides evidence for membrane-specific changes in the abundance of a number of other enzymes required for peptidoglycan biosynthesis. Four PBPs involved in the extracellular cross-link formation stage of mature peptidoglycan formation (SCO2608, SCO3157, SCO39010 and SCO4013) showed a 1.5–2-fold decrease in abundance in the membrane-associated fraction immediately following vancomycin addition (Figure 6a), while enzymes for the intracellular biosynthesis of peptidoglycan precursors increased by a similar amount (Figure 4). The latter observation suggests a recruitment of the precursor synthesis enzymes to the intracellular face of the membrane to accompany the up-regulation in production of D-Ala-D-Lac lipid II derivatives directed by the *van* resistance cluster enzymes, while the former is consistent with a release of membrane-bound PBPs into the extracellular space. Whether this is part of a process to clear damaged proteins from the membrane or part of a proactive process to help maintain or repair the peptidoglycan is an open question. The observation that Pbp2a (a homologue of SCO2608 Pbp2) from *Streptococcus pneumoniae* exists in two forms possessing different glycosyltransferase activities may support the latter proposal.⁴⁴ A truncated periplasmic form of Pbp2a synthesizes longer glycan chains than the full-length membrane-bound enzyme.

(ii). Metabolic Responses to Stress

The observed up-regulation of enzymes participating in the pentose phosphate shunt (GO: 0006098 $p = 3.46 \times 10^{-3}$) may serve to counteract the effect of production of reactive oxygen species (ROS) which often takes place following exposure to antimicrobial agents and which can be the ultimate cause of bacteriocidal activity in some circumstances.⁴⁵ In *E. coli* the ability to generate NADPH via the pentose phosphate pathway has been shown to form an important part of the cellular response to ROS stress induced following exposure to paraquat or tellurite.^{46–48} An increase in abundance of enzymes putatively involved in the synthesis and recycling of mycothiol, a buffering thiol metabolite with protective properties similar to glutathione (reviewed in Newton et al.⁴⁹), is also indicative of a need to deal with chemical damage, perhaps resulting from ROS generation, following exposure of cells to vancomycin. This increase was however specific to the membrane subproteome (Figure 6d) and suggests a localized need for the mycothiol activity. The mycothiol conjugate amidase (Mca) encoded by SCO4967 and up-regulated ~2-fold in the membrane subproteome is a key enzyme involved in mycothiol-dependent detoxification; deletion of Mca in

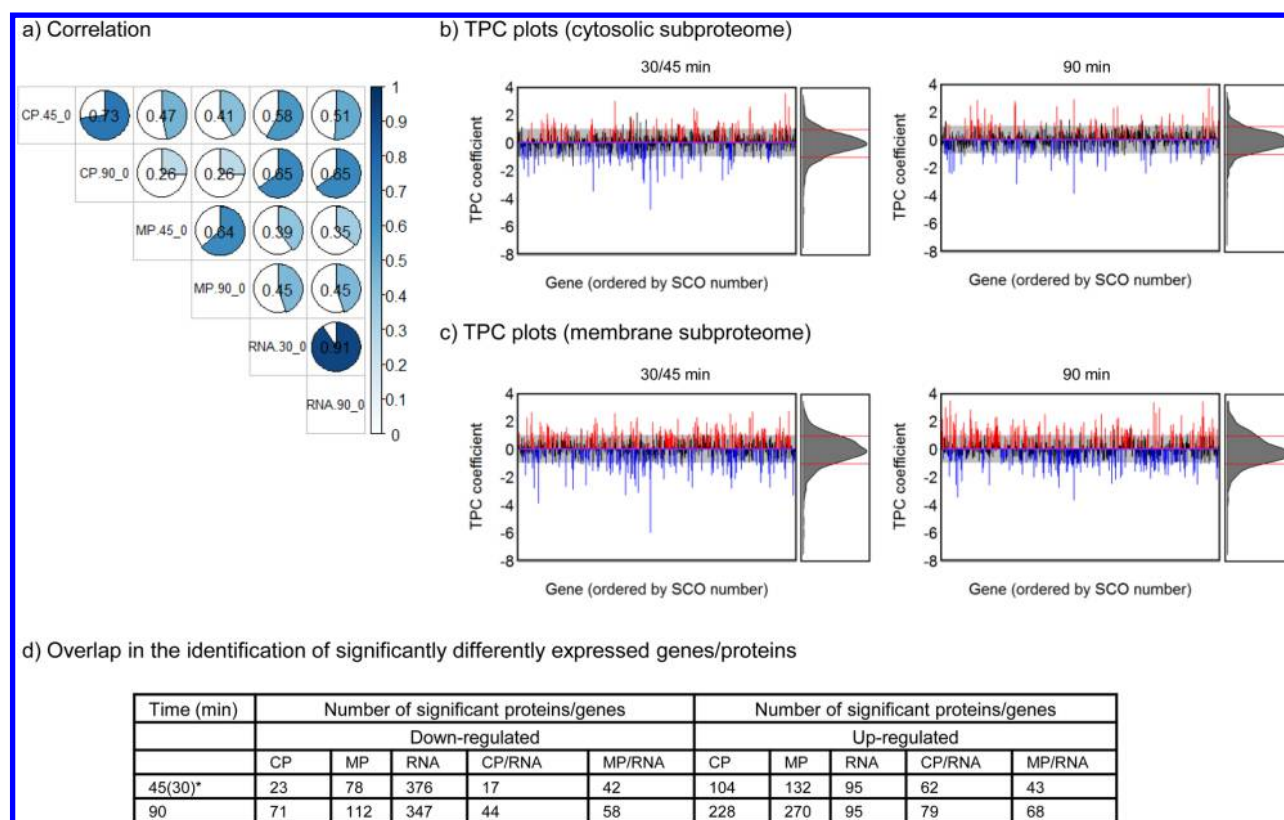


Figure 8. Contrasting the rate of change in abundance of proteins with transcripts in the response of *S. coelicolor* to vancomycin. (a) Pairwise Pearson correlation coefficients calculated from the common protein and transcript abundances (correlations shown were all significant to $p < 2.93 \times 10^{-13}$). (b) Transcript-protein congruence coefficients (TPC) calculated when comparing changes in mRNA levels with changes in abundance of proteins in the cytosolic subproteome. TPC values were calculated as described in the Supporting Methods. Genes with significantly ($p < 0.05$) higher or lower TPC values than 0 are indicated in red or blue, respectively. The panels to the right indicate the frequency distribution of the TPC coefficients that are shown in gene level detail in the main panels. The shaded rectangles and red dashed lines mark the range of TPC coefficients between -1 and $+1$, and since calculations are in the \log_2 scale correspond to genes encoding transcripts and proteins with relative changes in abundance differing by less than 2-fold. The panel to the left compares the 30 min transcriptome and 45 min proteome data, and the panel on the right compares the 90 min transcriptome and 90 min proteome data. (c) TPC coefficients similarly comparing changes in mRNA levels with changes in abundance of proteins in the membrane subproteome. (d) Overlap in the identification of significantly differently expressed genes between the proteome and transcriptome analysis platforms. CP = cytosolic protein fraction analysis; MP = membrane protein fraction analysis; RNA = transcriptome study; CP/RNA = gene identities shared between the cytosolic protein data and the transcriptome data; MP/RNA = gene identities shared between the membrane protein data and the transcriptome data; * denotes 45 min for the proteome samples and 30 min for the transcriptome samples.

Corynebacterium glutamicum has previously been shown to markedly increase sensitivity to vancomycin, lowering the MIC by 50%.⁵⁰

Enzymes required for the synthesis of the osmoprotective metabolite ectoine, normally associated with defense against high-salt environments, exhibited a marked increase in abundance that was restricted to the plasma membrane (Figure 6b). Interestingly, none of the enzymes encoded by the ectoine cluster are predicted from their sequence to be membrane localized (see Supporting File S2) and the mechanism for this spatial accumulation is therefore yet to be determined. Ectoine has recently been shown to stabilize the folding and enhance the stability of the model integral membrane protein bacterial rhodopsin⁵¹ and a role in promoting membrane protein stabilization during exposure to vancomycin is likely to be beneficial in preserving the functional integrity of the cell envelope. In addition to providing protection against the damaging effects of ROS, mycothiol also counteracts damage by nitric oxide⁴⁹ (NO). Proteins possessing 4Fe-4S clusters are a target for nitrosylation by NO^{52,53} and it is noteworthy that a group of seven iron sulfur proteins also exhibited a ~2-fold

increase in abundance in the membrane after vancomycin treatment (Figure 6b). These included two enzymes (SCO4550 and SCO4494) involved in the biosynthesis of menaquinone required for electron transfer and energy generation in the membrane (a third enzyme SCO4326 is similarly up-regulated (Supporting Figure S2)),⁵⁴ and also the NarG nitrate reductase SCO0216.⁵⁵ NarH (SCO0217) encoded by the same Nar2 locus was also identified as being increased in abundance at the membrane (Figure 6b) and while bacterial nitrate reductases are typically involved in energy generation under hypoxic conditions they have also been identified as sources of NO synthesis.^{56,57} NO is capable of protecting bacteria against the effects of a wide spectrum of antibiotics, in part by alleviating ROS-induced oxidative stress,⁵⁸ and it is possible that part of the response to vancomycin in *S. coelicolor* involves a Nar2-dependent membrane-localized synthesis of NO coincident with an increase in production of mycothiol and ectoine. The increase in the abundance of the menaquinone synthase and nitrate reductase enzymes also indicates a mechanism to boost plasma membrane energetics, perhaps to help compensate for the

observed depletion from the membrane of cytochrome oxidase (SCO2155 (Cox1)) and ATP synthase (SCO5369 (AtpF)) components identified among the group of proteins enriched in the cytosol (Figure 6c).

Four gene products belonging to a poorly characterized family of bacterial tellurium-resistance proteins were found to be up-regulated in the cytoplasm in response to vancomycin exposure (Figure 6c). LocateP predicts all to be localized intracellularly (see Supporting File S2). The tellurium oxyanion tellurite is highly toxic through its ability to cause oxidative stress and tellurium-resistance proteins are proposed to provide protection against cellular ROS damage by mechanisms yet to be properly defined (reviewed in Anantharaman et al.³⁴).

(iii). Proteolysis and Amino Acid Metabolism

Proteases play important roles in bacterial responses to a variety of stresses through their activity in degrading damaged proteins, releasing damaged proteins from the cell membrane and also through their influence on the abundance of proteins with regulatory functions. The observed up-regulation of enzymes with proteolytic functions in both the cytosol (GO: 0006508 $p = 6.36 \times 10^{-3}$) and membrane (GO: 0044257 $p = 2.46 \times 10^{-3}$) samples following vancomycin treatment is consistent with the need to clear damaged proteins being an integral part of coping with the presence of the antibiotic. Although an increase in abundance of enzymes from the major protease types was observed (SCO1644 PcrB 20S proteasome subunit; SCO1648 Arc AAA+ ATPase; SCO3373 ClpC Clp-family protease; SCO5285 Lon AAA+ ATPase), the Lon protease encoded by SCO5285 exhibited the greatest up-regulation (~4-fold in the cytoplasm; Supporting Figure S2) and is likely to play the most significant role. Three enzymes encoded by a four gene operon required for branched chain amino acid catabolism (SCO2776–79)⁵⁹ exhibited a ~2-fold increase in abundance in both the cytoplasmic and membrane-associated subproteomes following vancomycin addition (Supporting Figure S2), while arginine biosynthesis was a significantly enriched functional class among the proteins showing increased abundance in the cytoplasm (GO:00006526 $p = 4.59 \times 10^{-5}$; Figure 3). An up-regulation of arginine biosynthesis has previously been identified in a *femAB* mutant of *S. aureus* that is unable to form the correct crossbridges in cell wall peptidoglycan suggesting a link between this pathway and a weakened cell wall structure that is supported by the current study.⁶⁰ The change in arginine biosynthesis in *S. aureus* was attributed to creating an alternative pathway for ATP generation by increasing the conversion of carbamoylphosphate to carbamate. Arginine is however an important hub metabolite and in *S. coelicolor* its significance may be related to the observed increase in ectoine biosynthesis (via glutamate), or putatively in polyamine or proline synthesis for osmoprotection. The intracellular levels of both arginine and proline have been shown to increase markedly in a metabolomics analysis of the salt stress response in *S. coelicolor*.⁶¹ Up-regulation of branched chain amino acid catabolism could reflect the increased activity of the protein degradation machinery and subsequent channelling of the degradation products into energy generating pathways but might also be indicative of an increase in branched chain fatty acid biosynthesis to produce phospholipids for the plasma membrane which in *S. coelicolor* contain predominantly branched chain fatty acids.

(iv). Regulatory Proteins

In addition to the CseBC two-component regulatory system belonging to the cell envelope stress response signal transduction pathway a number of other gene products with known or predicted regulatory functions were identified as being significantly altered in abundance following vancomycin treatment (Figure 6a,b,e and Figure 7). These are likely to play roles in adapting to the stress induced by the antibiotic and include many predicted to be related to nucleotide sensing or synthesis. Two proteins with predicted cAMP binding domains, SCO0168 and the cAMP receptor protein Crp (SCO3571), were significantly up-regulated, the latter exclusively in the membrane-associated subproteome. SCO3352, a close homologue of the *Mycobacterium tuberculosis* cdiAMP synthetase enzyme DisA (61% amino acid identity, $E = 1 \times 10^{-140}$), increased in abundance in both proteome fractions following vancomycin treatment raising the possibility that cdiAMP signaling may play a role in the response to antibiotic stress. The GTP binding protein family was a significantly enriched functional class among the proteins showing increased abundance preferentially in the membrane fraction (GO:0005525 $p = 1.12 \times 10^{-3}$; Supporting Table S1 and Figure 6b) and included representatives of the Obg (SCO2595), Era (SCO2539) and EngA (SCO1758) GTPase families which cycle between off and on regulatory states dependent upon the binding of GDP or GTP, respectively.⁶² These GTPases play central roles in regulating bacterial cell growth potentially by fine-tuning fundamental cellular processes such as ribosome assembly to energy availability and status. Small regulatory GTPases of the RAS superfamily are present in each of the 13 conserved regions present in the genome of *S. coelicolor*⁶³ and sensor histidine kinases from three of these (Cvns 1, 10 and 13) decreased significantly in abundance after vancomycin treatment. Interestingly, the lone conserved region found in the related actinomycete *Mycobacterium smegmatis* has been shown to be involved in resistance to the antibiotic fluoroquinolone through its regulation of DNA gyrase.⁶⁴ Sensor protein kinases from both the histidine and Ser/Thr families were significantly altered in abundance in the membrane-associated subproteome after vancomycin treatment with inevitable downstream consequences on the signaling cascades that they control (Figures 6 and 7). Most of these signaling cascades have however yet to be defined and the significance in this context is therefore unclear. The functional consequences of the marked up-regulation in abundance of the principal sigma factor σ^{HrdD} are similarly largely unknown, although a recent functional genomics analysis of the changes taking place in the 6 h following spore germination in *S. coelicolor* observed that σ^{HrdD} is the most highly expressed sigma factor at this stage in the life cycle when cell wall restructuring and synthesis is a priority.⁶⁵ A cohort of 88 genes were predicted to be transcribed by σ^{HrdD} including those encoding the Lon and ClpB proteases discussed above, and 30 encoding gene products with regulatory functions (including 26 DNA-binding transcriptional regulators). This suggests a pivotal role for this sigma factor, itself regulated at the transcriptional level by the CseBC- σ^{E} cell envelope stress response signal transduction system, in coordinating the response to vancomycin.

■ CONCLUDING REMARKS

S. coelicolor possesses a cluster of seven *van* resistance genes known to confer inducible high level resistance to vancomycin via a mechanism involving a remodelling of peptidoglycan biosynthesis. It is however clear from the extensive temporal changes observed in the proteome following vancomycin treatment that the response to this antibiotic is considerably more complex than simple induction of expression of the enzymes encoded by the *van* resistance cluster, involving significant changes in the abundance of several hundred additional proteins. Importantly the data also indicate an extra layer of complexity in the response on the basis of changes in protein spatial localization whereby functionally related groups of proteins are recruited or depleted from the plasma membrane following vancomycin exposure. Analysis of the data in the context of known or predicted protein function annotations enabled the significance of many of the observed spatiotemporal changes in protein expression to be usefully interpreted, but we are still some way from obtaining a fully integrated understanding of how they contribute to preserving cell viability in the presence of vancomycin. The reliable detection of only 11% of the total theoretical proteome (from transcriptomics data we estimate ~50% of genes are expressed in the experimental conditions used) also set a limit to the knowledge obtainable. The results of the current analysis do however suggest a number of avenues for future study which should be revealing, and improvements in MS technology and sample preparation techniques promise greater coverage of the proteome in the future. It would be particularly interesting to define the contributions to the response to vancomycin that are dependent on the major regulatory proteins identified as significantly changing in abundance following treatment. Analysis of changes in the phosphoproteome to characterize the significance of the sensor kinase proteins which increase in abundance exclusively in the membrane-associated protein fractions in response to vancomycin, and identification of the regulons controlled by the σ^E and σ^{HrdD} sigma factors would both be useful approaches for further defining the global regulatory response. In addition to the appropriate regulation of gene expression the maintenance of plasma membrane energetics is crucial for cell survival under conditions of stress, and the putative roles of the increased abundance at the membrane of mycothiol and menaquinone biosynthesis enzymes and the Nar2 nitrate reductase complex in contributing to this (or to NO biosynthesis in the case of Nar2) is similarly of fundamental interest.

■ ASSOCIATED CONTENT

Supporting Information

Supporting File S1. Protein-level abundance data for the replicate experiments summarized in Table 1, plus normalized abundances for the 804 proteins common to all replicates. Supporting File S2. Localization scores and LocateP predictions to compare the predicted and observed cellular localizations for the 804 proteins quantified in the LC–MS/MS analysis. Supporting File S3. Proteins significantly differently expressed in *S. coelicolor* in the 90 min following exposure of exponentially growing liquid cultures to vancomycin. Supporting File S4. Hierarchical cluster groups for the proteins significantly differently expressed ($P < 0.05$) in *S. coelicolor* in the 90 min following exposure of exponentially growing liquid cultures to vancomycin. Supporting File S5. Contrasting the rate of change

in abundance of proteins in the cytosolic and membrane-associated subproteomes of *S. coelicolor* following exposure to vancomycin for 45 min. Supporting File S6. Contrasting the rate of change in abundance of proteins in the cytosolic and membrane-associated subproteomes of *S. coelicolor* following exposure to vancomycin for 90 min. Supporting File S7. Contrasting the rate of change in abundance of proteins in the cytosol with the rate of change of mRNA in the transcriptome data. Supporting File S8. Contrasting the rate of change in abundance of proteins in the membrane-associated samples with the rate of change of mRNA in the transcriptome data. Supporting File S9. Overlap in the identification of significantly differently expressed genes/proteins, as presented in Figure 8b. Supporting tables: Gene Ontology (GO) analysis results for (Table S1) the membrane enriched and membrane depleted protein categories identified in Figure 5; (Table S2) the cytosol enriched and cytosol depleted protein categories identified in Figure 5; (Table S3) the high-confidence set of vancomycin responsive genes identified in both the transcriptome and proteome studies. Supporting Figure S1: Localization score plots comparing scores at 0 min (immediately before vancomycin addition) with those calculated for samples (a) 45 min after treatment, and (b) 90 min after treatment. Figure S2: Mean normalized abundance profiles for selected groups of proteins discussed in the text. Supporting Methods provides greater detail for some of the data analysis procedures described in the Materials and Methods. The Supporting Information is available free of charge on the ACS Publications website at DOI: 10.1021/acs.jproteome.5b00242.

■ AUTHOR INFORMATION

Corresponding Authors

*E-mail: arh69@cam.ac.uk.

*E-mail: hh309@cam.ac.uk.

Notes

The authors declare no competing financial interest.

■ ACKNOWLEDGMENTS

This work has been supported by funds from the Royal Society (516002.K5877ROG) and the Medical Research Council (GO700141). We are grateful to members of the Cambridge Centre for Proteomics for technical support.

■ REFERENCES

- (1) Rybak, M.; Lomaestro, B.; Rotschafer, J.; Moellering, R.; Craig, W.; Billeter, M.; Dalovisio, J.; Levine, D. Vancomycin therapeutic guidelines: a summary of consensus recommendations from the infectious diseases Society of America, the American Society of Health-System Pharmacists, and the Society of Infectious Diseases Pharmacists. *Clin. Infect. Dis.* **2009**, *49* (3), 325–7.
- (2) Liu, C.; Bayer, A.; Cosgrove, S.; Daum, R.; Fridkin, S.; Gorwitz, R.; Kaplan, S.; Karchmer, A.; Levine, D.; Murray, B.; et al. Clinical practice guidelines by the infectious diseases society of america for the treatment of methicillin-resistant *Staphylococcus aureus* infections in adults and children. *Clin. Infect. Dis.* **2011**, *52* (3), e18–e55.
- (3) Rubinstein, E.; Keynan, Y. Vancomycin revisited—60 years later. *Front. Public Health* **2014**, *2*, 217.
- (4) Uttley, A. H.; George, R. C.; Naidoo, J.; Woodford, N.; Johnson, A. P.; Collins, C. H.; Morrison, D.; Gilfillan, A. J.; Fitch, L. E.; Heptonstall, J. High-level vancomycin-resistant enterococci causing hospital infections. *Epidemiol. Infect.* **1989**, *103* (1), 173–81.
- (5) Howden, B. P.; Davies, J. K.; Johnson, P. D.; Stinear, T. P.; Grayson, M. L. Reduced vancomycin susceptibility in *Staphylococcus aureus*, including vancomycin-intermediate and heterogeneous vanco-

mycin-intermediate strains: resistance mechanisms, laboratory detection, and clinical implications. *Clin. Microbiol. Rev.* **2010**, *23* (1), 99–139.

(6) Patel, R. Enterococcal-type glycopeptide resistance genes in non-enterococcal organisms. *FEMS Microbiol. Lett.* **2000**, *185* (1), 1–7.

(7) Hong, H.-J.; Hutchings, M. I.; Neu, J. M.; Wright, G. D.; Paget, M. S.; Buttner, M. J. Characterization of an inducible vancomycin resistance system in *Streptomyces coelicolor* reveals a novel gene (*vanK*) required for drug resistance. *Mol. Microbiol.* **2004**, *52* (4), 1107–21.

(8) Sosio, M.; Bianchi, A.; Bossi, E.; Donadio, S. Teicoplanin biosynthesis genes in *Actinoplanes teichomyeticus*. *Antonie van Leeuwenhoek* **2001**, *78* (3–4), 379–84.

(9) Sosio, M.; Stinchi, S.; Beltrametti, F.; Lazzarini, A.; Donadio, S. The gene cluster for the biosynthesis of the glycopeptide antibiotic A40926 by nonmuraraea species. *Chem. Biol.* **2003**, *10* (6), 541–9.

(10) Guardabassi, L.; Perichon, B.; Heijenoort, J.; Blanot, D.; Courvalin, P. Glycopeptide resistance *vanA* operons in paenibacillus strains isolated from soil. *Antimicrob. Agents Chemother.* **2005**, *49* (10), 4227–33.

(11) Marshall, C. G.; Lessard, I. A.; Park, I.; Wright, G. D. Glycopeptide antibiotic resistance genes in glycopeptide-producing organisms. *Antimicrob. Agents Chemother.* **1998**, *42* (9), 2215–20.

(12) Forsberg, K. J.; Reyes, A.; Wang, B.; Selleck, E. M.; Sommer, M. O.; Dantas, G. The shared antibiotic resistome of soil bacteria and human pathogens. *Science* **2012**, *337* (6098), 1107–11.

(13) Novotna, G.; Hill, C.; Vincent, K.; Liu, C.; Hong, H.-J. A novel membrane protein, VanJ, conferring resistance to teicoplanin. *Antimicrob. Agents Chemother.* **2012**, *56* (4), 1784–96.

(14) Kwun, M. J.; Novotna, G.; Hesketh, A. R.; Hill, L.; Hong, H.-J. In vivo studies suggest that induction of VanS-dependent vancomycin resistance requires binding of the drug to D-Ala-D-Ala termini in the peptidoglycan cell wall. *Antimicrob. Agents Chemother.* **2013**, *57* (9), 4470–80.

(15) Kwun, M. J.; Hong, H.-J. The activity of glycopeptide antibiotics against resistant bacteria correlates with their ability to induce the resistance system. *Antimicrob. Agents Chemother.* **2014**, *58* (10), 6306–10.

(16) Koteva, K.; Hong, H.-J.; Wang, X. D.; Nazi, I.; Hughes, D.; Naldrett, M. J.; Buttner, M. J.; Wright, G. D. A vancomycin photoprobe identifies the histidine kinase VanSsc as a vancomycin receptor. *Nat. Chem. Biol.* **2010**, *6* (5), 327–9.

(17) Hong, H.-J.; Hutchings, M. I.; Buttner, M. J. Vancomycin resistance VanS/VanR two-component systems. *Adv. Exp. Med. Biol.* **2008**, *631*, 200–13.

(18) Hong, H.-J.; Hutchings, M. I.; Hill, L. M.; Buttner, M. J. The role of the novel Fem protein VanK in vancomycin resistance in *Streptomyces coelicolor*. *J. Biol. Chem.* **2005**, *280* (13), 13055–61.

(19) Hesketh, A.; Hill, C.; Mokhtar, J.; Novotna, G.; Tran, N.; Bibb, M.; Hong, H.-J. Genome-wide dynamics of a bacterial response to antibiotics that target the cell envelope. *BMC Genomics* **2011**, *12*, 226.

(20) Liu, X.; Hu, Y.; Pai, P.-J.; Chen, D.; Lam, H. Label-free quantitative proteomics analysis of antibiotic response in *Staphylococcus aureus* to oxacillin. *J. Proteome Res.* **2014**, *13* (3), 1223–33.

(21) Hessling, B.; Bonn, F.; Otto, A.; Herbst, F.-A.; Rappen, G.-M.; Bernhardt, J.; Hecker, M.; Becher, D. Global proteome analysis of vancomycin stress in *Staphylococcus aureus*. *Int. J. Med. Microbiol.* **2013**, *303* (8), 624–34.

(22) Lin, X.; Kang, L.; Li, H.; Peng, X. Fluctuation of multiple metabolic pathways is required for *Escherichia coli* in response to chlortetracycline stress. *Mol. Biosyst.* **2014**, *10* (4), 901–8.

(23) Kim, D.; Chater, K. F.; Lee, K. J.; Hesketh, A. Effects of growth phase and the developmentally significant *bldA*-specified tRNA on the membrane-associated proteome of *Streptomyces coelicolor*. *Microbiology* **2005**, *151* (8), 2707–20.

(24) Kessner, D.; Chambers, M.; Burke, R.; Agus, D.; Mallick, P. ProteoWizard: open source software for rapid proteomics tools development. *Bioinformatics* **2008**, *24* (21), 2534–6.

(25) Holman, J. D.; Tabb, D. L.; Mallick, P. Employing ProteoWizard to convert raw mass spectrometry data. *Curr. Protoc. Bioinf.* **2014**, *46*, 13.24.1–9.

(26) Brosch, M.; Yu, L.; Hubbard, T.; Choudhary, J. Accurate and sensitive peptide identification with Mascot Percolator. *J. Proteome Res.* **2009**, *8* (6), 3176–81.

(27) Shadforth, I. P.; Dunkley, T. P.; Lilley, K. S.; Bessant, C. i-Tracker: for quantitative proteomics using iTRAQ. *BMC Genomics* **2005**, *6*, 145.

(28) Zhou, M.; Boekhorst, J.; Francke, C.; Siezen, R. LocateP: Genome-scale subcellular-location predictor for bacterial proteins. *BMC Bioinf.* **2008**, *9* (1), 173.

(29) Smyth, G. K. Limma: linear models for microarray data. In *Bioinformatics and Computational Biology Solutions using R and Bioconductor*; Springer: New York, 2005; Vol. XIX, pp 397–420.

(30) Bauer, S.; Grossmann, S.; Vingron, M.; Robinson, P. N. Ontologizer 2.0—a multifunctional tool for GO term enrichment analysis and data exploration. *Bioinformatics* **2008**, *24* (14), 1650–1.

(31) Thompson, A.; Schäfer, J.; Kuhn, K.; Kienle, S.; Schwarz, J.; Schmidt, G.; Neumann, T.; Johnstone, R.; Mohammed, A. K.; Hamon, C. Tandem mass tags: a novel quantification strategy for comparative analysis of complex protein mixtures by MS/MS. *Anal. Chem.* **2003**, *75* (8), 1895–904.

(32) Kahne, D.; Leimkuhler, C.; Lu, W.; Walsh, C. Glycopeptide and lipoglycopeptide antibiotics. *Chem. Rev.* **2005**, *105* (2), 425–48.

(33) Manteca, A.; Sanchez, J.; Jung, H. R.; Schwämmle, V.; Jensen, O. N. Quantitative proteomics analysis of *Streptomyces coelicolor* development demonstrates that onset of secondary metabolism coincides with hypha differentiation. *Mol. Cell Proteomics* **2010**, *9* (7), 1423–36.

(34) Anantharaman, V.; Iyer, L. M.; Aravind, L. Ter-dependent stress response systems: novel pathways related to metal sensing, production of a nucleoside-like metabolite, and DNA-processing. *Mol. Biosyst.* **2012**, *8* (12), 3142–65.

(35) Chandra, G.; Chater, K. F. Developmental biology of *Streptomyces* from the perspective of 100 actinobacterial genome sequences. *FEMS Microbiol. Rev.* **2014**, *38* (3), 345–79.

(36) Fernández Martínez, L.; Bishop, A.; Parkes, L.; del Sol, R.; Salerno, P.; Sevcikova, B.; Mazurakova, V.; Kormanec, J.; Dyson, P. Osmoregulation in *Streptomyces coelicolor*: modulation of SigB activity by OsaC. *Mol. Microbiol.* **2009**, *71* (5), 1250–62.

(37) Derouaux, A.; Dehareng, D.; Lecocq, E.; Halici, S.; Nothaft, H.; Giannotta, F.; Moutzourelis, G.; Dusart, J.; Devreese, B.; Titgemeyer, F.; et al. Crp of *Streptomyces coelicolor* is the third transcription factor of the large CRP-FNR superfamily able to bind cAMP. *Biochem. Biophys. Res. Commun.* **2004**, *325* (3), 983–90.

(38) Piette, A.; Derouaux, A.; Gerkens, P.; Noens, E. E. E.; Mazzucchelli, G.; Vion, S.; Koerten, H. K.; Titgemeyer, F.; Pauw, E. De; Leprince, P.; et al. From dormant to germinating spores of *Streptomyces coelicolor* A3(2): new perspectives from the *crp* null mutant. *J. Proteome Res.* **2005**, *4* (5), 1699–708.

(39) Paget, M. S.; Chamberlin, L.; Atrih, A.; Foster, S. J.; Buttner, M. J. Evidence that the extracytoplasmic function sigma factor sigmaE is required for normal cell wall structure in *Streptomyces coelicolor* A3(2). *J. Bacteriol.* **1999**, *181* (1), 204–11.

(40) Hong, H.-J.; Paget, M. S.; Buttner, M. J. A signal transduction system in *Streptomyces coelicolor* that activates the expression of a putative cell wall glycan operon in response to vancomycin and other cell wall-specific antibiotics. *Mol. Microbiol.* **2002**, *44* (5), 1199–211.

(41) Paget, M. S.; Leibovitz, E.; Buttner, M. J. A putative two-component signal transduction system regulates sigmaE, a sigma factor required for normal cell wall integrity in *Streptomyces coelicolor* A3(2). *Mol. Microbiol.* **1999**, *33* (1), 97–107.

(42) Manteca, A.; Jung, H. R.; Schwämmle, V.; Jensen, O. N.; Sanchez, J. Quantitative proteome analysis of *Streptomyces coelicolor* nonsporulating liquid cultures demonstrates a complex differentiation process comparable to that occurring in sporulating solid cultures. *J. Proteome Res.* **2010**, *9* (9), 4801–11.

(43) Eymann, C.; Dreisbach, A.; Albrecht, D.; Bernhardt, J.; Becher, D.; Gentner, S.; Tam, L. T. e T.; Büttner, K.; Buurman, G.; Scharf, C.;

et al. A comprehensive proteome map of growing *Bacillus subtilis* cells. *Proteomics* **2004**, *4* (10), 2849–76.

(44) Helassa, N.; Vollmer, W.; Breukink, E.; Vernet, T.; Zapun, A. The membrane anchor of penicillin-binding protein PBP2a from *Streptococcus pneumoniae* influences peptidoglycan chain length. *FEBS J.* **2012**, *279* (11), 2071–81.

(45) Kohanski, M. A.; Dwyer, D. J.; Hayete, B.; Lawrence, C. A.; Collins, J. J. A common mechanism of cellular death induced by bactericidal antibiotics. *Cell* **2007**, *130* (5), 797–810.

(46) Rui, B.; Shen, T.; Zhou, H.; Liu, J.; Chen, J.; Pan, X.; Liu, H.; Wu, J.; Zheng, H.; Shi, Y. A systematic investigation of *Escherichia coli* central carbon metabolism in response to superoxide stress. *BMC Syst. Biol.* **2010**, *4*, 122.

(47) Shen, T.; Rui, B.; Zhou, H.; Zhang, X.; Yi, Y.; Wen, H.; Zheng, H.; Wu, J.; Shi, Y. Metabolic flux ratio analysis and multi-objective optimization revealed a globally conserved and coordinated metabolic response of *E. coli* to paraquat-induced oxidative stress. *Mol. Biosyst.* **2013**, *9* (1), 121–32.

(48) Sandoval, J. M.; Arenas, F. A.; Vásquez, C. C. Glucose-6-phosphate dehydrogenase protects *Escherichia coli* from tellurite-mediated oxidative stress. *PLoS One* **2011**, *6* (9), e25573.

(49) Newton, G. L.; Buchmeier, N.; Fahey, R. C. Biosynthesis and functions of mycothiol, the unique protective thiol of Actinobacteria. *Microbiol. Mol. Biol. Rev.* **2008**, *72* (3), 471–94.

(50) Si, M.; Long, M.; Chaudhry, M. T.; Xu, Y.; Zhang, P.; Zhang, L.; Shen, X. Functional characterization of *Corynebacterium glutamicum* mycothiol S-conjugate amidase. *PLoS One* **2014**, *9* (12), e115075.

(51) Roychoudhury, A.; Bieker, A.; Häussinger, D.; Oesterhelt, F. Membrane protein stability depends on the concentration of compatible solutes—a single molecule force spectroscopic study. *Biol. Chem.* **2013**, *394* (11), 1465–74.

(52) Crack, J. C.; Smith, L. J.; Stapleton, M. R.; Peck, J.; Watmough, N. J.; Buttner, M. J.; Buxton, R. S.; Green, J.; Oganessian, V. S.; Thomson, A. J.; et al. Mechanistic insight into the nitrosylation of the [4Fe-4S] cluster of WhiB-like proteins. *J. Am. Chem. Soc.* **2011**, *133* (4), 1112–21.

(53) Crack, J. C.; Stapleton, M. R.; Green, J.; Thomson, A. J.; Brun, N. E. Le. Mechanism of [4Fe-4S](Cys)₄ cluster nitrosylation is conserved among NO-responsive regulators. *J. Biol. Chem.* **2013**, *288* (16), 11492–502.

(54) Hiratsuka, T.; Furihata, K.; Ishikawa, J.; Yamashita, H.; Itoh, N.; Seto, H.; Dairi, T. An alternative menaquinone biosynthetic pathway operating in microorganisms. *Science* **2008**, *321* (5896), 1670–3.

(55) Fischer, M.; Alderson, J.; van Keulen, G.; White, J.; Sawers, R. G. The obligate aerobe *Streptomyces coelicolor* A3(2) synthesizes three active respiratory nitrate reductases. *Microbiology (Reading, U. K.)* **2010**, *156* (Pt 10), 3166–79.

(56) Vine, C. E.; Purewal, S. K.; Cole, J. A. NsrR-dependent method for detecting nitric oxide accumulation in the *Escherichia coli* cytoplasm and enzymes involved in NO production. *FEMS Microbiol. Lett.* **2011**, *325* (2), 108–14.

(57) Corker, H.; Poole, R. K. Nitric oxide formation by *Escherichia coli*. Dependence on nitrite reductase, the NO-sensing regulator Fnr, and flavohemoglobin Hmp. *J. Biol. Chem.* **2003**, *278* (34), 31584–92.

(58) Gusarov, I.; Shatalin, K.; Starodubtseva, M.; Nudler, E. Endogenous nitric oxide protects bacteria against a wide spectrum of antibiotics. *Science* **2009**, *325* (5946), 1380–4.

(59) Zhang, Y. X.; Denoya, C. D.; Skinner, D. D.; Fedechko, R. W.; McArthur, H. A.; Morgenstern, M. R.; Davies, R. A.; Lobo, S.; Reynolds, K. A.; Hutchinson, C. R. Genes encoding acyl-CoA dehydrogenase (AcdH) homologues from *Streptomyces coelicolor* and *Streptomyces avermitilis* provide insights into the metabolism of small branched-chain fatty acids and macrolide antibiotic production. *Microbiology (Reading, U. K.)* **1999**, *145* (Pt 9), 2323–34.

(60) Hübscher, J.; Jansen, A.; Kotte, O.; Schäfer, J.; Majcherczyk, P. A.; Harris, L. G.; Bierbaum, G.; Heinemann, M.; Berger-Bächi, B. Living with an imperfect cell wall: compensation of *femAB* inactivation in *Staphylococcus aureus*. *BMC Genomics* **2007**, *8*, 307.

(61) Kol, S.; Merlo, M. E.; Scheltema, R. A.; de Vries, M.; Vonk, R. J.; Kikkert, N. A.; Dijkhuizen, L.; Breitling, R.; Takano, E. Metabolomic characterization of the salt stress response in *Streptomyces coelicolor*. *Appl. Environ. Microbiol.* **2010**, *76* (8), 2574–81.

(62) Caldon, C. E.; March, P. E. Function of the universally conserved bacterial GTPases. *Curr. Opin. Microbiol.* **2003**, *6* (2), 135–9.

(63) Wuichet, K.; Søgaard-Andersen, L. Evolution and diversity of the Ras superfamily of small GTPases in prokaryotes. *Genome Biol. Evol.* **2015**, *7* (1), 57–70.

(64) Tao, J.; Han, J.; Wu, H.; Hu, X.; Deng, J.; Fleming, J.; Maxwell, A.; Bi, L.; Mi, K. Mycobacterium fluoroquinolone resistance protein B, a novel small GTPase, is involved in the regulation of DNA gyrase and drug resistance. *Nucleic Acids Res.* **2013**, *41* (4), 2370–81.

(65) Strakova, E.; Zikova, A.; Vohradsky, J. Inference of sigma factor controlled networks by using numerical modeling applied to microarray time series data of the germinating prokaryote. *Nucleic Acids Res.* **2014**, *42* (2), 748–63.